

Use of in-fiber Bragg grating sensors to measure PDL strain in an ex-vivo swine model

Leigh Armijo

A thesis
submitted in partial fulfillment of the
requirements for the degree of

Master of Science in Dentistry

University of Washington
2021

Committee:

Tracy Popowics

Sue Herring

Anne-Marie Bollen

Katherine Rafferty

Program Authorized to Offer Degree:

Orthodontics

© Copyright 2021

Leigh Armijo

University of Washington

Abstract

Use of in-fiber Bragg grating sensors to measure PDL strain in an ex-vivo swine model

Leigh Armijo

Chair of the Supervisory Committee:

Dr. Tracy Popowics
Oral Health Sciences

Although in-fiber Bragg grating (FBG) sensors have been used to measure strain within the PDL in a swine model, how fluid movement and collagen deformation contribute to these measurements remain unknown. The purpose of this study is to determine whether FBG sensors detect changes within the PDL of ex-vivo swine tooth-PDL-bone complex (TPBC) samples when manipulating fluid flow and fiber content. Being able to record strain will allow a better understanding of the biomechanics of viscoelastic load transfer from the tooth to the PDL that lead to orthodontic tooth movement. FBG sensors placed within the PDL of swine incisor teeth were used to measure strain resulting from an intrusive load applied by an MTS machine and compared between varying conditions: dry vs. saline (n=19) and saline vs. collagenase and fiberotomy (n=11). Saline samples resulted in greater strain values than collagenase-treated, whereas dry and saline did not statistically differ. The dry and collagenase-treated strain and force values were more consistent than the saline. There was also a downward trend in measured force values for the saline and collagenase-treated specimens that was not noticed in the dry sample. Further studies will lead to more precise and controlled tooth movement as we gain knowledge of the required forces needed to induce adequate strain on the PDL for remodeling. In conclusion, the FBG sensors were able to detect fluid and fibrous changes within the PDL environment, and both seem to be involved in determining strain in response to loading.

INTRODUCTION

The periodontal ligament (PDL) is a supporting structure that bridges the gap between alveolar bone and cementum of teeth, comprised primarily of collagenous type I and type III fibers surrounded by an extracellular matrix (Berkovitz, 1990). The extracellular matrix contains a compilation of cells including endothelial cells, epithelial rests of Malassez, cementoblasts and others. The predominant cell type is fibroblasts, which make up about 25% of the PDL cells in humans. These cells are rich in cytoplasmic microfilament systems which aid in contraction and movement (Al-Rekabi et al., 2019). The PDL is characterized with a high remodeling capacity as it is exposed to constant stresses (Beertsen et al., 1997).

These constant stresses and rapid turnover have led to the basis of orthodontic tooth movement in which with an applied load, bone resorption occurs at compressive sides and bone deposition at tension sides (Henneman et al., 2008). Applied load causes strain, including fluid flow in the PDL and alveolar bone, and leads to PDL fibroblast and osteocyte cell deformation. Cell strain activates osteocytes in the canaliculi of alveolar bone and stimulates osteoblast and osteoclast differentiation (Henneman et al., 2008). Stretching of PDL on the tension side stimulates osteoblastic bone formation and compressive loading on the opposing side leads to osteoclastic bone resorption. Thus, the mechanical forces applied to a tooth and the resulting PDL and bone remodeling result in the movement of teeth within the alveolar bone (Kitaura et al., 2014).

The RANKL-OPG pathway has been found to have a key role in the alveolar changes associated with orthodontic tooth movement. For example, compressive forces result in the increased expression of RANKL and decreased expression of OPG by

osteoblasts and PDL cells, promoting osteoclast differentiation from monocytes (Zhang et al., 2016). Osteoclast resorption of bone creates space for the tooth to move into (Kohara et al., 2012). Within the PDL, fibroblasts and osteoblasts produce matrix metalloproteinases and cathepsins which stimulate extracellular matrix degradation on the side of compression (Takahashi et al., 2003 and 2006). Under tensile forces, osteoblasts and PDL cells upregulate OPG and decrease expression of RANKL leading to the reduction in osteoclast activity and an increase in osteogenesis by osteoblasts (Jacobs et al., 2013). Collagen within the PDL aligns along the direction of tensile force resulting in osteoblasts filling up the space vacated by the tooth with new bone (Komatsu et al., 2007a).

Previous studies on PDL responses to applied load have been performed. One approach is to isolate the PDL by cutting a section from the tooth-PDL-bone complex (TPBC) and clamping the connected bone and tooth to test the PDL alone (Komatsu et al., 2007b; Toms et al., 2002). This method allows direct measure of the response of mechanical stress to the PDL, but limits understanding of its interaction with surrounding bone and tooth. Another method uses the PDL intact in the TPBC and applies displacement force on the tooth and measures changes due to applied load over time (Papadopoulou et al., 2013; Wei et al., 2014). This second method uses a reverse finite element analysis (FEA) which assumes a given model to calculate the changes in PDL. However, due to the complex structure and components of the PDL, model validation specifically for PDL has not yet been accomplished (Natali et al., 2004).

The disadvantages of the previous methods have led to an alternative method of the use of in-fiber Bragg grating (FBG) sensors to measure PDL response under applied

load in a TPBC (Romanyk et al., 2017). The FBG sensors were first discovered by Ken Hill in 1978 and have since the 1990s been developed for commercial use for a wide variety of sensing applications in telecommunication, aeronautics, automotive technology, civil engineering and other industries. The FBG sensors have an intrinsic capability to measure multiple parameters, including strain, temperature, and pressure (Cusano et al., 2011). The small size, biocompatibility, chemical inertness, and high resolution of FBG sensors have demonstrated their biomechanical use in ex-vivo pressure mapping in orthopedic joints, stress in intervertebral discs, forces induced by tendons and ligaments, and many other applications (Al-Fakih et al., 2012).

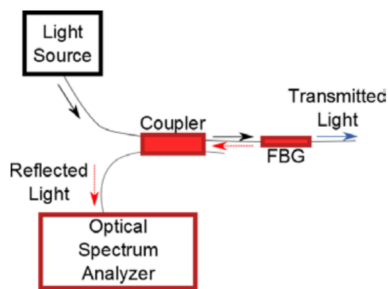


Figure 1. Schematic of FBG operation (Romanyk et al., 2017)

The FBG sensor, which measures 1mm in length and 0.125mm in diameter, is contained in an optical fiber (Measures, 2001). Coupling the FBG embedded in the optical fiber, light from a broadband source results in the optical fiber reflecting a portion of the transmitted light to the FBG sensing unit, the Bragg wavelength, which is measured by an optical spectrum analyzer (Figure 1; Al-Fakih et al., 2012). When the FBG sensor is subjected to an external mechanical load, a shift in peak wavelength results due to a change in the amount of reflected light and using the gauge factor of $-1.21\text{pm}/\mu\epsilon$, wavelength shift can be converted to strain (Measures, 2001).

Previous studies have investigated the viscoelastic biomechanics within the PDL by altering fluid and fiber content. In a rat model with collagenase-treated PDL, the stress-relaxation process showed collagenase-treated specimens relaxed more rapidly than the control due to decreased quantity and organization of collagen fibers (Komatsu, 2010). In video-recorded images of bovine samples submerged in a saline bath undergoing compression, the PDL appeared as a porous matrix in which fluid can freely flow in and out of the ligament space during compressive and tensile loading phases (Bergomi et al., 2010). In another bovine model using saline saturated and partially dry samples, liquid was shown to be a major contributor to the PDL's resistance to compression. Removing this fluid component largely eliminates the PDL's damping effect in compression (Bergomi et al., 2010B). While Romanyk, et al. have shown that repeatable PDL strain measures on saline saturated swine TPBC can be achieved with FBG sensors, the biological mechanisms that are occurring remain unknown (e.g. fluid movement, collagen deformation, etc.). Further study is needed to determine whether the FBG sensors can detect PDL strains that correspond with the orthodontic forces that lead to tooth movement, making them a potential option for future ex-vivo and in-vivo studies.

The use of mechanics in orthodontics involves reloading of force on teeth over a period of time until resultant tooth movement has occurred. Orthodontic tooth movement to achieve an ideal occlusion and esthetics can be met with complications as there is a balance between too little force where minimal to no movement occurs and too much stress that can lead to detrimental effects on roots of teeth and their alveolar housing. Multiple studies have looked into the adverse effects of orthodontic tooth movement,

including hyalinization, orthodontic induced root resorption and PDL necrosis (Maeda et al., 2015; Viecilli et al., 2013; Quinn and Yoshikawa, 1985; Cheng et al., 2009; Brezniak and Wasserstein, 1993). High force application leads to greater PDL stress and correlates with increased external root resorption (Cheng et al., 2009). Not only increased stress, but also treatment time (Brezniak and Wasserstein, 1993), magnitude of stimulus and individual susceptibility (Viecilli et al., 2009) lead to increased orthodontic external root resorption. PDL necrosis can result in reduction in root length, compromised prosthetic support, mobility and in extreme cases tooth loss (Levander et al., 2000). These studies have shown that tooth movement and forces applied to teeth have limits and understanding the positive and negative effects on the PDL, bone and tooth can help reduce harmful and potentially irreversible outcomes, like tooth loss. Being able to accurately and precisely measure strain within the PDL on experimental subjects will allow a better understanding of optimal force levels and lead to more efficiency in orthodontic tooth movement.

The pig, *Sus scrofa*, has been shown to be a viable model for the human masticatory apparatus. Pigs have a comparable growth pattern to humans and show similarities in physiology of mastication, jaw movements and hard palate (Oltramari et al., 2007). As omnivorous creatures, similar to humans, the teeth exhibit function consistent with the incisors being used for cutting and premolars and molars for grinding food (Popowics et al., 2004). Pigs are often used due to similarity in tooth size and function to humans and relatively easy access to the mouth and teeth for research purposes (Oltramari et al., 2007). Indeed, previous work has used pigs to model traumatic intrusive forces on mandibular incisors (Patterson and Popowics, 2014). While the

current research study is focusing primarily on mandibular incisors ex-vivo, a future goal is to implement FBG sensors in-vivo, and in a live pig, the mandibular incisors are the most accessible teeth.

The PDL, with its small size and complex structure, makes studying the mechanics of this tissue and its role in tooth movement difficult. Without a better understanding of strain in the PDL, the limits of force that may be applied to a tooth without adverse effects remain unknown. The purpose of this study is to determine whether in-fiber Bragg grating (FBG) sensors detect changes within the PDL of ex-vivo swine tooth-PDL-bone complex (TPBC) samples when manipulating fluid flow and fiber content. Another purpose is to look at the force levels needed to intrude an incisor tooth to a predetermined depth with intermittent loading of the samples with varying fluid flow and fiber content. As a future goal is to implement this technique in live animals, evaluating the variability of FBG strain measurements within a tooth and between examiners will be used to evaluate repeatability in methodology. In order to better understand the biomechanics of viscoelastic load transfer from the tooth to the PDL that lead to orthodontic tooth movement, the objectives for this project are:

1. Use in-fiber Bragg grating (FBG) sensors to measure PDL strain when manipulating fluid content using saline within the PDL space of swine tooth-PDL-bone complex (TPBC) undergoing a 0.5mm repetitive intrusive load
2. Use FBG sensors to measure PDL strain when manipulating fiber content within the PDL space with a fiberotomy and collagenase incubation in swine TPBC undergoing a 0.5mm repetitive intrusive load

3. Compare MTS force values required for a 0.5mm intrusive repetitive load when manipulating fluid and fiber content in incisor swine TPBC
4. Compare the repeatability of FBG strain and MTS force values measured between younger and older age groups of swine incisors in saline condition undergoing a 0.5mm intrusive load
5. Compare interexaminer repeatability of FBG strain measurements for the younger incisor saline group undergoing a 0.5mm intrusive load
6. Evaluate trends of FBG strain and MTS force values over repeated 0.5mm intrusive load of swine incisors under the varying fluid and fiber conditions

METHODS

Sample size

This study obtained 13 pig mandibles, approximately 2 months of age (younger group), in primary dentition. Each was sectioned to isolate the anterior region containing the deciduous canines and incisor teeth (Figure 2). For some incisors from the younger group, instability of the incisors within the alveolar housing following collagenase incubation occurred; thus, 5 pig mandibles, approximately 4 months of age (older group) of larger size, in primary dentition were obtained for the collagenase tests. The older group pig specimens were more robust and are expected to have greater PDL fiber density, alveolar bone density and longer root length, maintaining greater stability following the collagenase incubation (Tonge and McCance, 1973). All pig mandibles were obtained postmortem from the University of Washington paramedical training program or a local butcher, so no ethical conflicts were encountered. Both central

incisors per mandible, when available, housed in their alveolar complex were used to compare for controlled varying conditions: 1) dry vs. saline solution, 2) saline vs. saline with fibrotomy and collagenase incubation (Table 1).

Table 1. Number of samples with varying conditions, pig age, and examiner.

| Condition | Dry (younger - Examiner 1) | Saline (younger- Examiner 1) | Saline (younger - Examiner 2) | Saline w/ collagenase (younger- Examiner 2) | Saline (older- Examiner 2) | Saline w/ collagenase older- Examiner 2) |
|---------------------|----------------------------|------------------------------|-------------------------------|---|----------------------------|--|
| Number of incisors | 19 | 19 | 4 | 4 | 7 | 7 |
| Number of mandibles | 10 | 10 | 3 | 3 | 5 | 5 |

Sample Size Calculation

The key variable in this study is viscoelastic change in the PDL by manipulating fluid and fiber content. Although the FBG sensors have been used to measure strain within swine PDL previously, they have not been used to investigate strain under different fluid and fiber conditions. Previous studies have recorded the stress-relaxation of periodontal tissues in different fluid environments, however, there are no studies measuring strain readings associated with fluid changes in the PDL. For the median maximum peak strain and peak force, a sample size of 16 incisors per condition was determined to have 80% power to demonstrate a difference equal to $\frac{3}{4}$ the standard deviation between conditions, based on a two-sample t-test at a 0.05 significance level. Preliminary data from 2 incisors indicated the distribution of the outcomes could be skewed, hence the sample size was increased to 19 incisors per condition for dry vs. saline tests based on the maximum number of incisors available. For the collagenase treated specimens, a convenience sample of 11 incisors was used as availability of the pigs was more limited and therefore the saline vs. collagenase group was underpowered.

Apparatus and Procedures

The mandibular central incisor tooth segments were harvested and stored frozen for preservation in 0.9% saline solution. Samples, when ready to be tested, were thoroughly thawed in saline and mounted in a dental plaster stone base. The incisal edges of the central incisors were ground flat using a dental handpiece and carbide bur to reduce breakage and provide a more even loading surface.

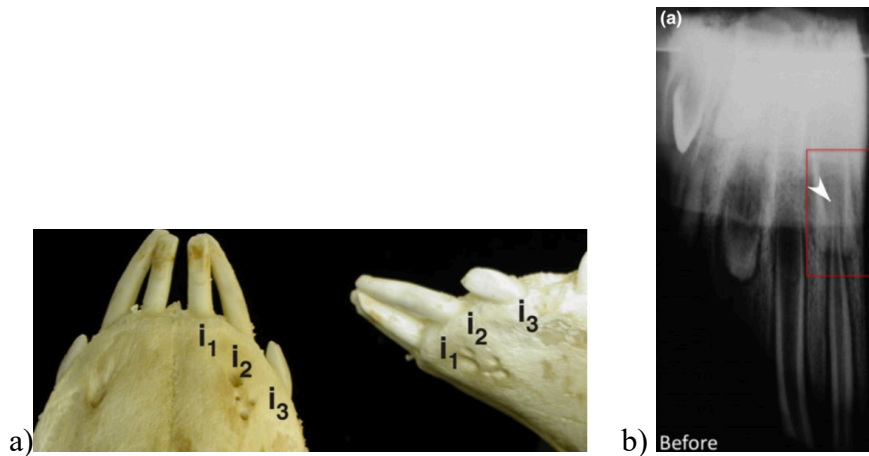


Figure 2. a) Primary swine incisors from facial and lateral views, central incisor (i1) is being used in this study, b) Periapical radiograph of approximate 5-6 month old anterior pig mandible in primary dentition showing closed apex of the primary incisor and developing succeeding tooth (Patterson and Popowics, 2014)

The mounted specimens were placed in a watertight chamber on the adjustable mounted frame. The loading platen was centered on the incisal edge oriented perpendicularly to the estimated long axis of the tooth. It was predetermined whether dry or saline condition would be tested first to allow a nearly balanced number of samples beginning with the same condition. To avoid drying and wetting the sample's PDL multiple times, both incisors per mandible were tested either both dry or both in saline first. For the saline-saturated conditions, the testing chamber was filled with saline to the level just above the marginal gingiva to allow liquid flow within the PDL but with the incisal edge exposed for force application; the specimen was allowed to equilibrate for 15

minutes prior to testing. Five specimens of the younger pigs were tested in saline by a second examiner to evaluate repeatability and trends. Five mandibles of the older pigs were used to compare saline-saturated with and without a fiberotomy performed of the gingival and alveolar crest fibers using a surgical blade. The saline condition was performed first in all of these comparative trials as a fiberotomy was expected to change the amount of fluid flow within the PDL. To ensure adequate breakdown of the collagen fibers, following the saline test, a collagenase solution (24units/ml PBS) was injected into the periodontal space where the fiberotomy was performed and the specimen was incubated for 4 hours at 37° C (Komatsu et al., 2007a and Komatsu, 2010).

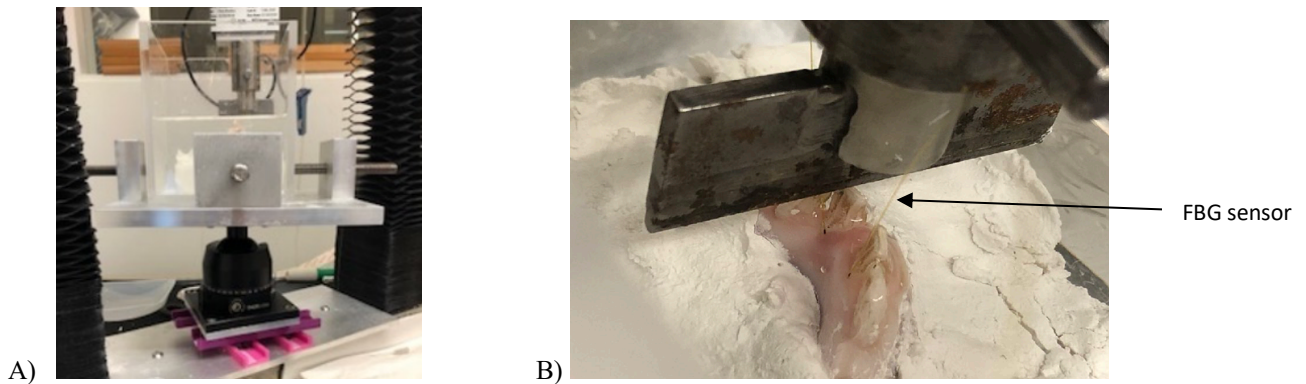


Figure 3. A) Customized submersion chamber containing anterior pig mandible with saline, fixed in place on an adjustable mounting stage below the MTS loading platen. B) Mounted incisor in plaster with FBG sensor placed within the lingual PDL space to a marked 10mm depth

A materials testing machine (MTS SINTECH_2-S) was used to apply a compressive incisal load in an apical direction to the crown to intrude it. An adaptable mounting stage held the specimen stable in a customized submersion chamber for varying conditions (Figure 3). The FBG sensors were attached to a SmartScan Interrogator (SmartScan Dynamic FBG Interrogator, SmartFibers Ltd., Brachnell UK) to generate output data. For FBG sensor placement, a 27-gauge needle was inserted into the PDL from the gingival sulcus along the lingual tooth surface to a premeasured and marked 10mm depth which was maintained constant for all samples. The sensor was inserted through the

bore of the needle and the needle was carefully removed, leaving the FBG sensor in place within the PDL space at a 10mm depth from the lingual gingival margin. When both central incisors from one mandible were tested, two separate FBG sensors were inserted, one per tooth, prior to specimen placement into the liquid chamber. The sensors were maintained within the PDL space at the controlled depth for both dry and saline tests alternating which sensor was plugged into the SmartScan as each incisor data collection was performed separately. For the saline vs. collagenase tests, the FBG sensor was removed following the saline test to allow fiberotomy and collagenase incubation and reinserted for the post-collagenase test. The lingual insertion, as opposed to buccal, was used due to easier access and visualization from the angulation of the incisor crowns that will be used for future in-vivo testing.

The FBG sensor placement was tested by applying a load to the tooth and ensuring the SmartScan Interrogator produced an adequate microstrain output. For the dry vs. saline tests, once the FBG sensor placement was confirmed to be within the PDL space of each incisor, using a separate sensor per tooth, the sensors were not moved between the conditions. The adjustable platform moved the mandible specimen from one central incisor to its adjacent partner in a horizontal x-axis, not y or z, to minimize change in the incisor position relative to the loading platen. If the dry condition was tested first, each central incisor was tested 15 times with a 0.5N preload to a depth of 0.5mm at a speed of 0.3mm/s, followed by a 10s hold at the same depth, with 1-minute wait between trials. Once both incisors were tested dry, saline was added to the chamber to a level above the gingival margin but below the incisal edge, allowed to equilibrate for 15 minutes and each tooth retested 15 times with a 0.5N preload to a depth of 0.5mm at a

speed of 0.3mm/s, followed by a 10s hold at the same depth, with a 5-minute wait between trials. This longer wait time between reps for the saline tests is to allow saline to flow back into the PDL space as liquid had been expelled out due to the compressive load. If the saline tests were completed first, removal of the saline was performed using a pipette to draw the liquid out of the chamber without having to move the platform or FBG sensors and then each incisor was tested in the dry condition. Following the saline reps and removal of saline from the liquid chamber, the first 5 dry reps were used to “dry” the specimens with the assumption that any residual fluid was expelled from the PDL space during the initial reps.

For the older specimens testing saline vs. saline with fiberotomy and collagenase, the FBG placement was confirmed as previously stated. The saline condition was tested first for all 11 incisors for a total of 15 reps with a 0.5N preload to a depth of 0.5mm at a speed of 0.3mm/s with 5-minute wait between each trial. The FBG sensors were then removed from the lingual PDL space and a circumferential fiberotomy was performed using a 15c surgical blade. The collagenase solution was injected within the PDL space around the entire tooth using a syringe and allowed to incubate 4 hours at 37° C. Following incubation, the specimen was placed saturated in saline in the refrigerator overnight. The next day, the fiberoptic sensor was re-inserted in the lingual PDL to a depth of 10mm and testing of saline with fiberotomy and collagenase was completed for 15 reps with a 0.5N preload to a depth of 0.5mm at a speed of 0.3mm/s with a 5-minute wait between reps.

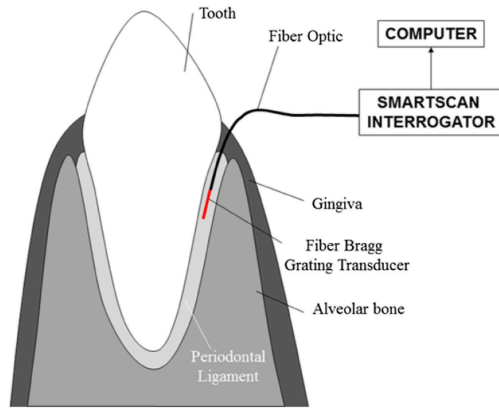
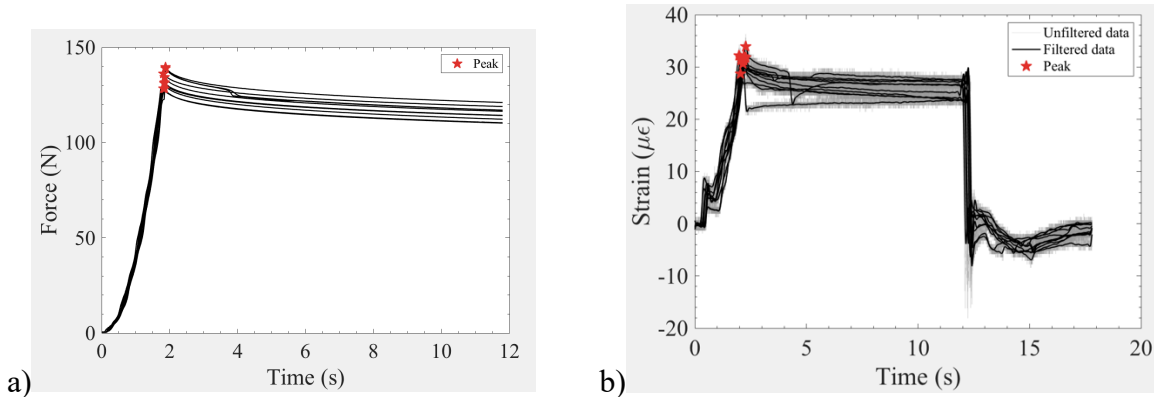


Figure 4. a) Diagram of FBG placement within the PDL (Romanyk et al. 2017).

When a load is applied to the tooth, the FBG sensor undergoes a shift in the Bragg wavelength detected by the SmartScan. Peak wavelength data were collected at 250 Hz using a 4th order Butterworth filter with a cutoff frequency of 50 Hz (Figure 4). The FBG SmartFiber software and MTS Testworks software were used to collect strain and force data, respectively, using a macro to standardize the time delay in program activation. Matlab (MathWorks, Natick, MA) software was used to convert the shift in Bragg wavelength to microstrain with a gauge factor of $-1.21 \text{ pm}/\mu\epsilon$ and identify the peak strain and force values (Measures, 2001). An output positive strain value indicates compression and a negative value indicates tension, which varied depending on incisor positioning relative to the loading platen (Figure 5).



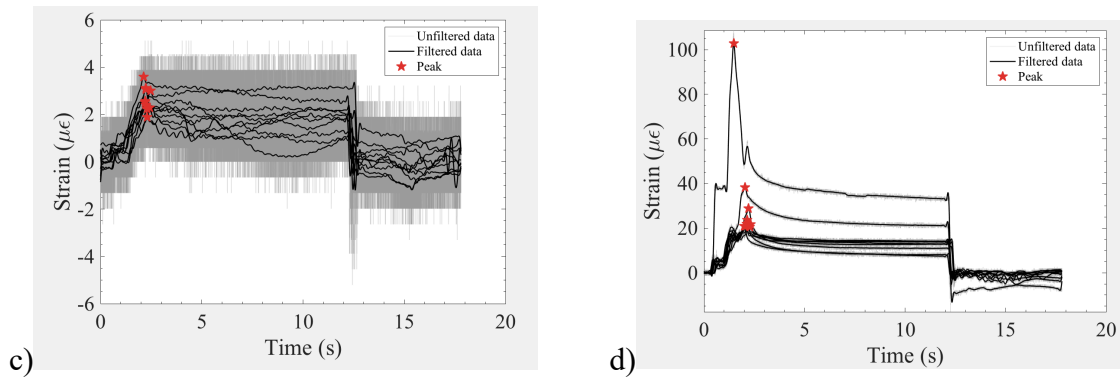


Figure 5. Examples of Matlab graph outputs depicting peak values of Force (a) and Strain (b) from reps 6-15, c) example of strain graph with greater noise, d) example of strain graph with outliers

DATA ANALYSIS

To control for outliers, the median instead of the mean value of maximum peak strain and force were obtained. To compare the maximum peak strain for the dry vs. saline data, the absolute value of the difference between testing conditions was used in order to treat strain due to compression and tension equally. These values always had the same polarity (compression or tension) for both conditions per given tooth. However, for the saline vs. collagenase data, polarity was maintained, because many of the samples shifted from compression to tension when collagenase/fibrotomy was applied. The tension strain readings obtained from a compressive applied load is likely due to tipping of the tooth instead of pure intrusion. First, the median of reps 6 to 15 was computed by run (a run consists of measurements taken on the same incisor) and condition and the difference bias-corrected bootstrap 95% confidence interval (CI) for the median of the differences between medians of dry and saline were computed based on 10,000 replications for each bootstrap CI. The first 5 reps were excluded to allow for preconditioning of the specimens.

The median absolute deviation about the median, also called median absolute deviation, was used to describe the repeatability (variability) of the maximum peak strain and peak force. The median absolute deviation (MAD) is given by

$$\text{MAD} = \text{median}(|X_i - \text{median}(X)|)$$

where i indexes the reps and $i = 6$ to 15 . To compare the repeatability between the dry and saline conditions, first the difference in the MAD value between the two conditions within the same run was computed to account for the positioning effect. Then the median of the differences in the MAD between the two conditions and bias-corrected bootstrap 95% confidence interval (CI) for the median of the differences between MADs was computed based on 10,000 replications for each bootstrap CI (Canty, 2019 & Davison, 1997).

To evaluate if the repeatability of the peak strain and peak force measurements varied over reps 6 to 15, the absolute deviation from the median within a trial (a trial consisted of 15 reps of one of the conditions on one incisor of one mandible) was computed for each observation and plotted against the rep number by condition. A loess smooth based on all trials was computed to summarize the trends over reps (Fig. 11, shown in blue) and a 95% confidence band for the overall smooth (shown in gray). Non-parametric smoothers like loess try to find a curve of best fit without assuming the data must fit some distribution shape (Cleveland, 1979).

For each condition, linear regression was used to test if there was a change in the repeatability of the peak strain or peak force over reps 6 to 15 by first testing for a quadratic trend, and if not significant, testing for a linear trend. To account for clustering of 10 repeated measurements within a trial, the linear regression was fit using generalized

estimating equations (Hardin, 2003 & Højsgaard, 2006). If there were outliers, the scatter plots truncated outliers in order to better display the trends in the data. The linear regression analysis was run with and without outliers. R-squared was used to describe the amount of the variation over reps 6 to 15 that could be attributed to a quadratic effect or a linear effect.

To evaluate if the maximum peak strain and peak force varied over reps 6 to 15, an analysis similar to the analysis for the repeatability was performed based on the deviation, instead of the absolute deviation, from the median within a trial. All analyses were performed using R statistical software (R Core Team, 2020).

Comparison by age

Table 2. Differences by age (older-younger) in the repeatability (MAD) and median peak strain and peak force.

| | Differences by age (older-younger) Median (95% CI) |
|---------------------------------------|--|
| Peak strain, MAD ($\mu\epsilon$) | -0.42 (-1.87, 0.78) |
| Peak force, MAD (N) | -0.11 (-4.48, 0.81) |
| Peak strain, median ($\mu\epsilon$) | -4.91 (-26.44, 7.85) |
| Peak force, median (N) | 15.02 (-64.74, 75.10) |

Table 2 summarizes the comparison between the two age groups of pigs for the repeatability and median maximum peak strain and peak force. The comparisons are restricted to runs using the saline condition only. There were no significant differences between runs using the two age groups in the repeatability or median levels for peak

strain and for peak force or their respective MAD values, therefore the younger and older samples were pooled in the saline vs. collagenase analysis.

Comparison of saline condition between Examiner 1 and Examiner 2

Table 3. Differences by examiner in the repeatability (MAD) and median peak strain and peak force.

| Study | N | Strain MAD ($\mu\epsilon$) Median (95% CI) | Force MAD (N) Median (95% CI) |
|--------------|----|---|----------------------------------|
| Examiner 2 | 9 | 1.33 (0.54, 2.20) | 2.81 (2.14, 4.90) |
| Examiner 1 | 19 | 0.72 (0.34, 0.92) | 2.33 (1.63, 2.70) |
| Examiner 2-1 | | 0.61 (-0.34, 1.73) | 0.48 (-0.66, 3.21) |

Table 3 compares the peak strain and force MAD values of the younger specimens undergoing saline condition testing based on 9 incisors from Examiner 2 and 19 incisors from Examiner 1. There was not a significant difference in the repeatability (MAD) for peak strain or for peak force between the two studies indicating reproducibility in methodology of FBG fiber placement and strain readings.

RESULTS

Comparison by condition

Comparison of fiberoptic measurements for dry vs saline

Table 4. Differences by condition (dry – saline) of the median for peak strain and peak force.

| | N | Differences by condition (Dry – Saline) Median (95% CI) |
|---------------------------------------|----|---|
| Peak strain, median ($\mu\epsilon$) | 19 | -0.82 (-2.96, 0.11) |
| Peak force, median (N) | 19 | 0.87 (-5.24, 5.98) |

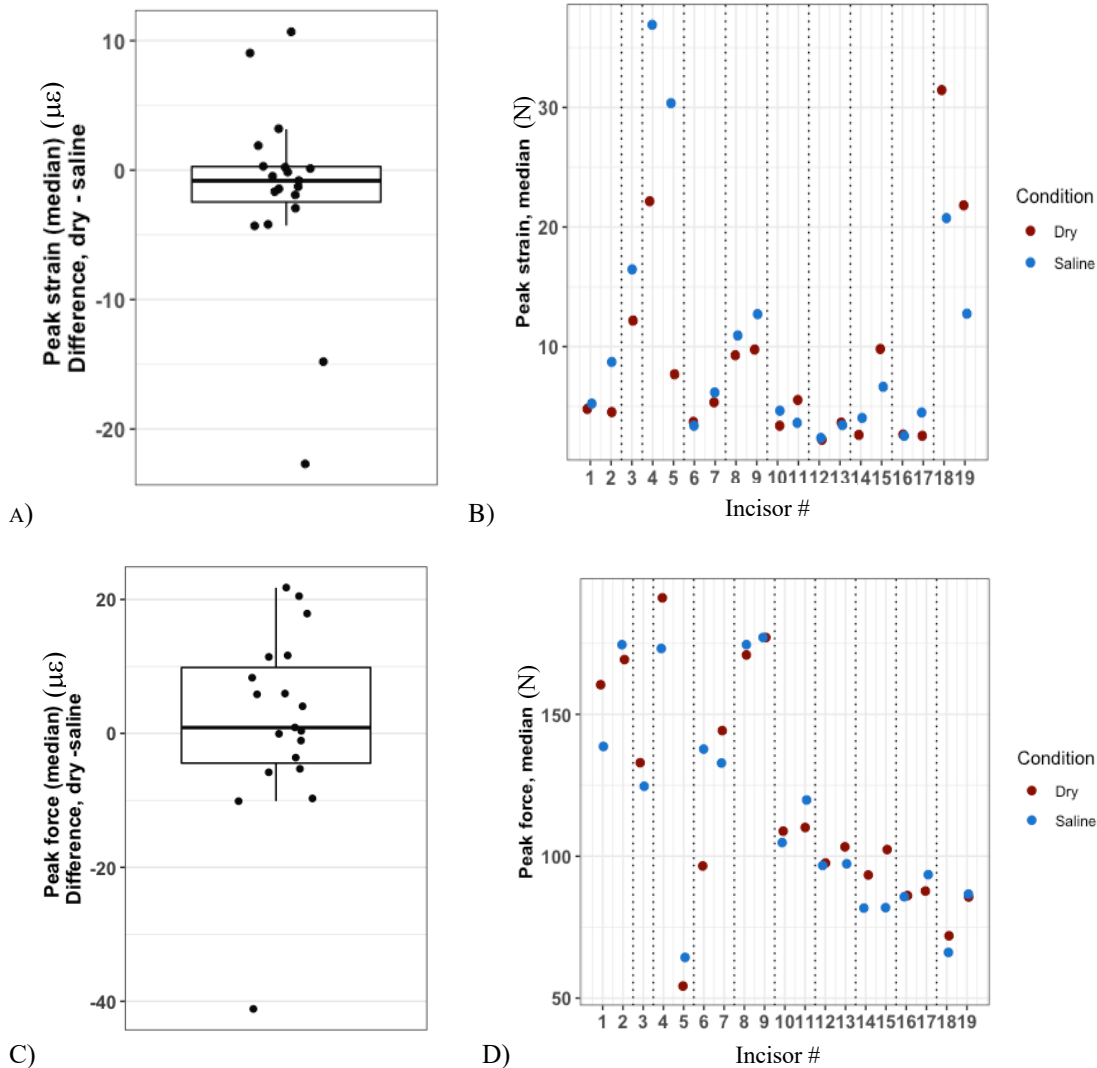


Figure 6. Difference between conditions (dry – saline) in the median peak strain and force
 A and C) Boxplot of the differences between the dry and saline conditions within each run for the younger group. A negative difference indicates the median strain (A) or force (C) was larger for the saline condition as compared to the dry condition. B and D) Scatter plot of the median for the dry and saline conditions by run, dashed vertical lines separate the different mandibles

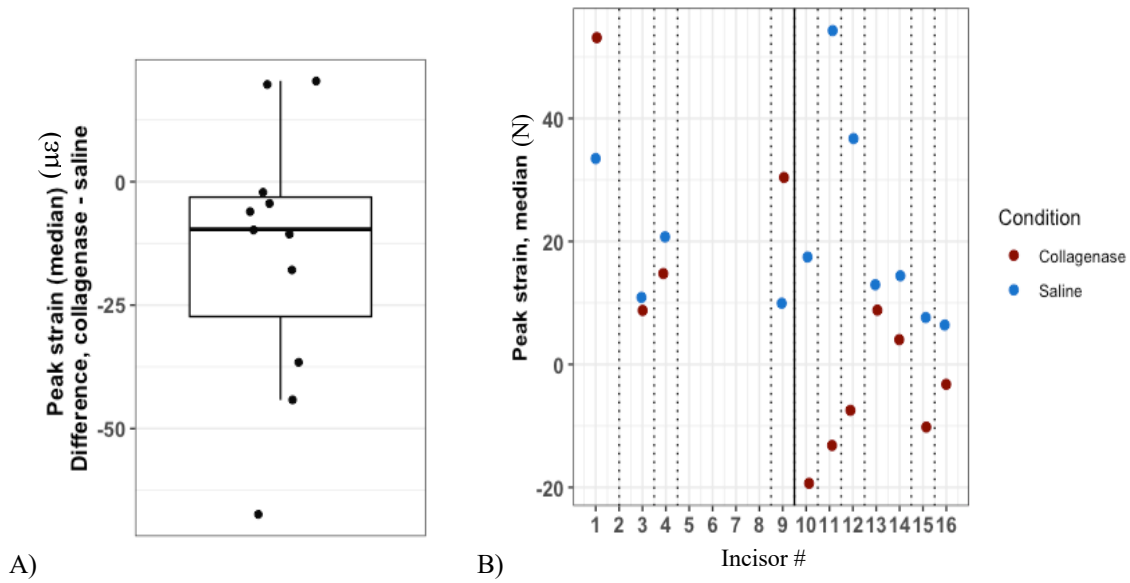
Median peak strain and force levels were compared between the dry and saline conditions in order to assess the effect of changes in the fluid environment. Overall, there was no significant difference in the median peak strain and median peak force levels between the dry and saline conditions (Table 2, Figure 6). However, given the upper bound of 95% CI for the median for the peak strain is near zero, almost negative, there

may be a tendency for median peak strain to be lower for the dry condition as compared to the saline conditions.

Comparison of fiberoptic measurements for saline vs. collagenase

Table 5. Differences by condition (saline w/ collagenase-saline) of the median for peak strain and peak force.

| | N | Differences by condition (Collagenase-Saline) Median (95% CI) |
|---------------------------------------|----|---|
| Peak strain, median ($\mu\epsilon$) | 11 | -9.63 (-44.21, -4.13) |
| Peak force, median (N) | 11 | -9.74 (-46.7, 4.62) |



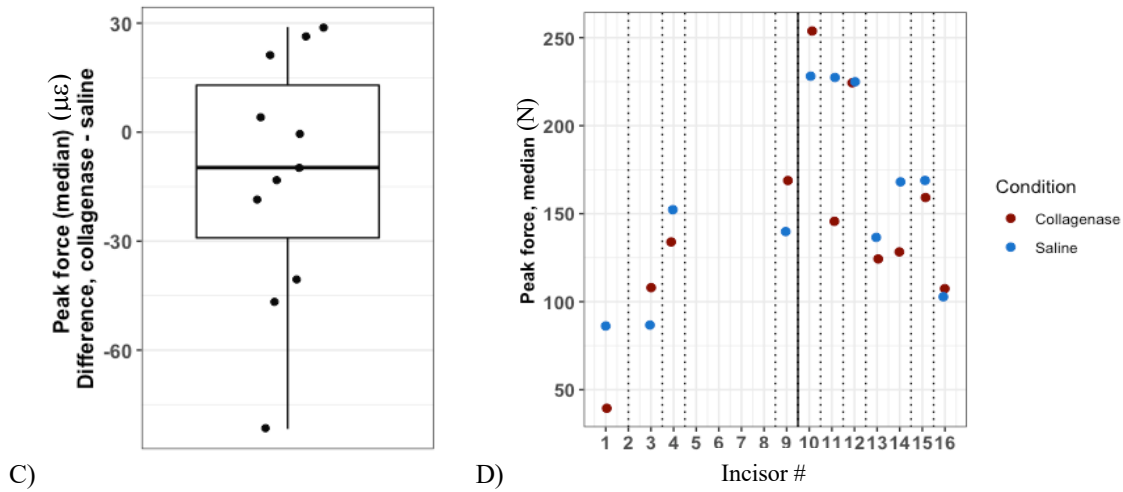


Figure 7. Difference between conditions (collagenase – saline) in the median peak strain
 A and C) Boxplot of the differences between the saline and saline conditions within each run. A negative difference indicates the median value was larger for the saline condition as compared to the collagenase condition. B and D) Scatter plot of the median for the collagenase and saline conditions by run, dashed vertical lines separate the different mandibles, solid vertical line separates younger and older mandibles (older are runs 10 to 16).

Median peak strain and force levels were also compared between the saline and the collagenase/fiberotomy conditions in order to assess the effect of changes in the integrity of PDL fibers on these measurements. As noted in the data analysis, the younger and older specimens that underwent saline and collagenase testing were pooled for N=11. This comparison demonstrated that the saline condition resulted with greater maximum peak strain values, however no difference in the peak force values was noted (Table 3, Figure 7).

Evaluating repeatability in measured strain and force over reps 6-15

Comparison by order dry vs. saline

Table 6. Evaluating repeatability of Peak strain, force and their respective MAD values by order run

| | N | Differences by order (1 st - 2 nd) Median (95% CI) |
|--|----|---|
| Peak strain, MAD ($\mu\epsilon$) | 19 | -0.02 (-0.47, 0.06) |
| Peak force, MAD (N) | 19 | -0.22 (-1.34, -0.01) |
| Peak strain, median ($\mu\epsilon$) | 19 | 1.65 (-0.45, 2.96) |
| Peak force, median (N) | 19 | 4.04 (-1.02, 5.85) |

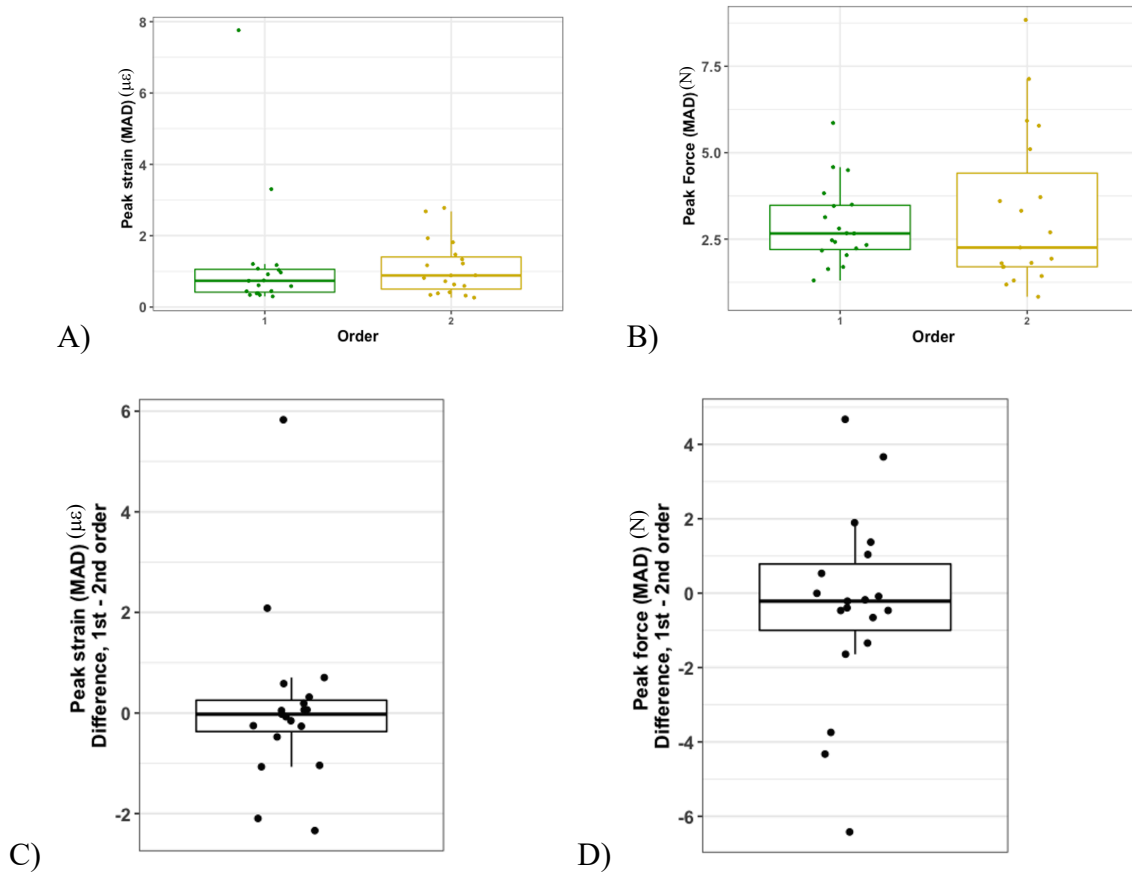


Figure 8. Boxplots by order run of strain (A) and force (B) and the difference between orders (1st-2nd) in the peak strain MAD (C) and peak force MAD (D)

The repeatability of peak strain and force measurements was assessed in order to determine the extent to which differences in the order of testing or fluid conditions affected these measurements. The effect of the order of testing on the peak values and repeatability, the median and MAD was compared (Table 4, Figure 8). Of the 19 incisors from the younger specimens that underwent dry vs. saline conditions, the order was nearly equal with 10 incisors undergoing dry testing first, and 9 undergoing saline first. The repeatability of the peak force was significantly better for the 1st set of reps as compared to the 2nd set of reps, regardless of testing condition. There is no strong evidence of a difference by order for peak strain given the 95% CI for the difference contains 0. Although the difference by order for the repeatability of the peak strain was not significant, there is some evidence that the repeatability was better for the 1st set of reps as compared to the 2nd set of reps (given the upper bound of the 95% CI is near zero, almost negative). There were no significant differences in the median levels between the 1st set of reps and 2nd set of reps.

Comparison by condition

Table 7. Evaluating repeatability using MAD values for Peak Strain and Peak Force based on condition (dry vs. saline)

| | N | Differences by condition (dry-saline) Median (95% CI) |
|------------------------------------|----|---|
| Peak strain, MAD ($\mu\epsilon$) | 19 | 0.06 (-1.04, 0.25) |
| Peak force, MAD (N) | 19 | 0.18 (-0.53, 1.04) |

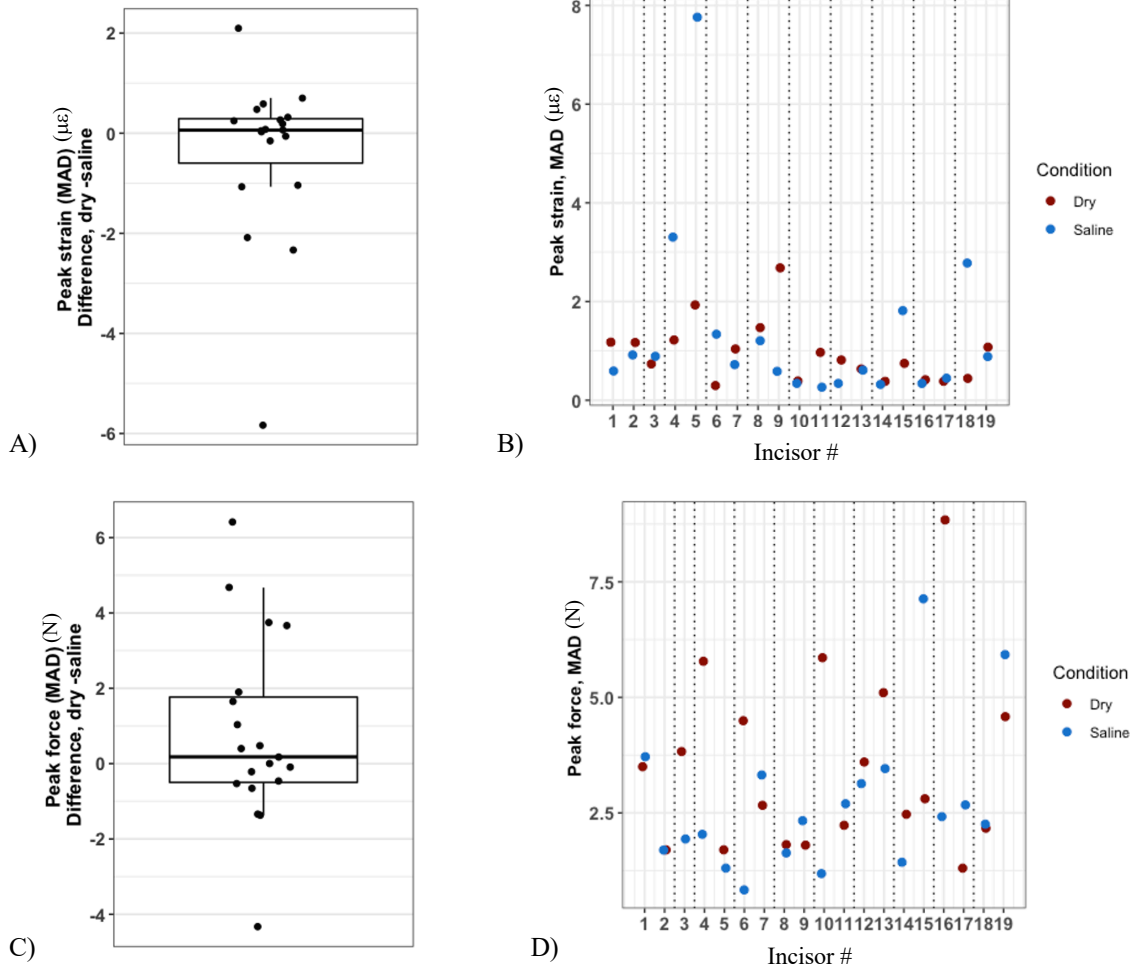


Figure 9. Difference between conditions (dry – saline) in the MAD of the median peak strain and force
 A and C) Boxplot of the differences between the dry and saline conditions MAD value within each run. A negative difference indicates the median value was larger for the saline condition as compared to the dry condition. B and D) Scatter plot of the median MAD for the dry and saline \

Next the effect of the fluid environment on repeatability of peak strain and force values, using MAD, was compared. The 95% CI for the median difference between MAD for peak strain in the dry and saline conditions within the same run contain the value zero, so there is no strong evidence of a difference in the repeatability between the dry and saline conditions (Table 5, Figure 9). However, the upper bound is near zero, almost negative, so there may be a tendency for the repeatability of peak strain to be better (smaller MAD) for the dry condition as compared to the saline condition. The 95% CI

for the median difference between MAD for peak force includes the value of zero, so differences in the repeatability between the dry and saline conditions were not observed.

Table 8. Evaluating repeatability using MAD values for Peak Strain and Peak Force based on condition (collagenase vs. saline)

| | N | Differences by condition (collagenase - saline) Median (95% CI) |
|------------------------------------|----|---|
| Peak strain, MAD ($\mu\epsilon$) | 11 | -0.31 (-1.42, 0.23) |
| Peak force, MAD (N) | 11 | 0.85 (-1.89, 1.28) |

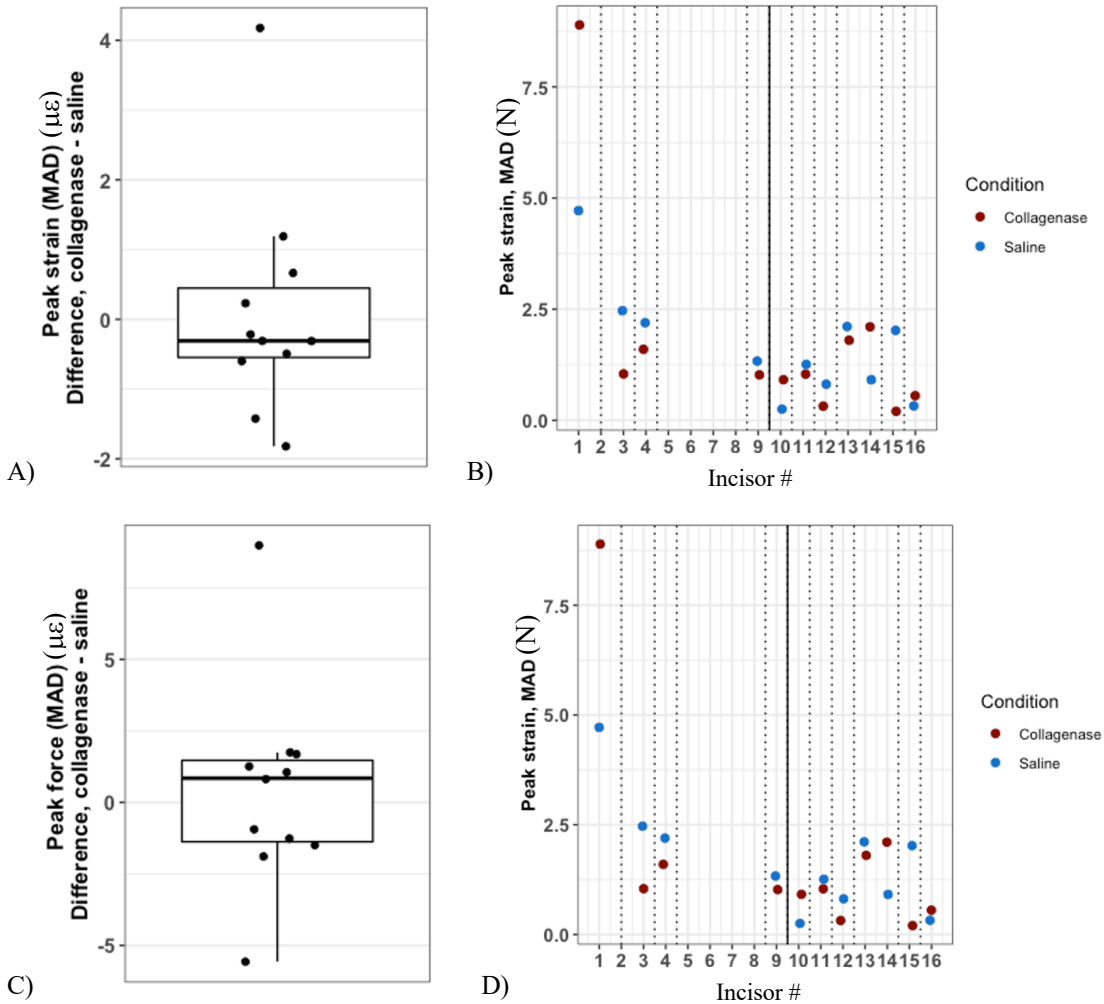


Figure 10. Difference between conditions (collagenase – saline) in the MAD of the median peak strain and force A and C) Boxplot of the differences between the collagenase and saline conditions MAD value within

each run. A negative difference indicates the median value was larger for the saline condition as compared to the collagenase condition. B and D) Scatter plot of the median MAD for the collagenase and saline conditions by run. Dashed vertical lines separate the different mandibles, solid vertical line separates younger and older mandibles (older are runs 10 to 16).

The effect of the integrity of the PDL fibers on repeatability of peak strain and force values was also compared using MAD. The 95% CI for the median difference between MAD strain for the collagenase and saline conditions within the same run contains the value zero, so there is no strong evidence of a difference in the repeatability between the collagenase and saline conditions (Table 6, Figure 10). However, the upper bound is near zero, almost negative for strain, so there may be some evidence that the repeatability of peak strain was better (smaller MAD) for the collagenase condition as compared to the saline condition. The 95% CI for the median force MAD difference includes the value of zero, so there is no strong evidence of difference in repeatability between the collagenase and saline conditions.

Evaluating trends in measured strain and force over reps 6-15

Trends over reps 6-15 in the repeatability of peak strain and peak force

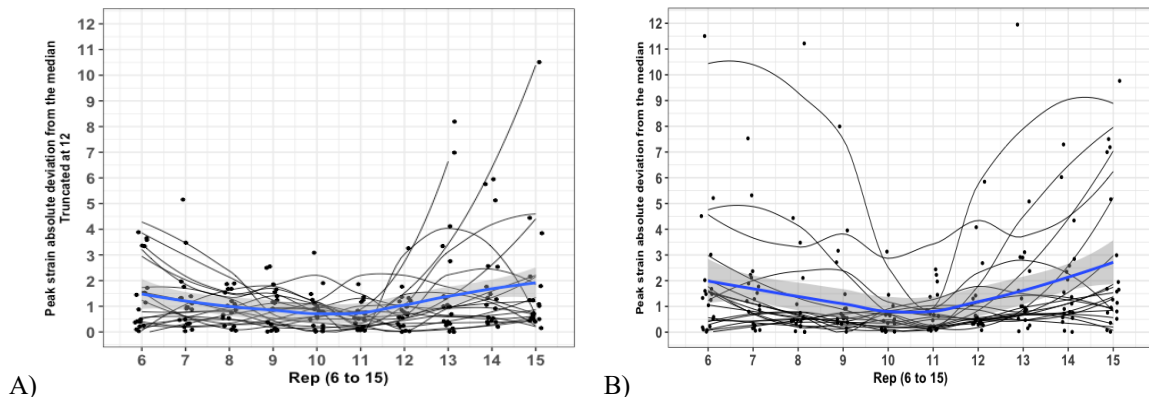


Figure 11. Trend in the absolute deviation around the median for **peak strain** over reps 6 to 15 for the **dry condition** – truncated figure (A) and **saline condition** (B)

Figure 11 shows the trends for the absolute deviation around the median for peak strain in the dry and saline conditions. Based on maximum peak strain dry test truncated data (N = 188 observations), there was a significant quadratic trend over reps 6 to 15 (p-value = 0.024; R-squared = 6.5%). After removing the 2 outliers there is some evidence of change in the repeatability over reps with the repeatability being better around reps 10 and 11 and worst at reps 6-7 and reps 14-15 for the dry condition. Based on all maximum peak strain saline test data from Examiner 1 (N = 190 observations as there were no extreme outliers), there was a significant quadratic trend over reps 6 to 15 (p-value = 0.008; R-squared = 6.8%), however it is difficult to determine if the magnitude of the change is relevant. The absolute deviation around the median is smallest (1.0) around runs 10 and 11, but higher at runs 6 and 14 and 15 (2 to 2.7). This quadratic only accounts for 6.8% of the variation over the 10 reps. Therefore, there is some evidence of change in the repeatability over reps with the repeatability being better around reps 10 and 11 and worst at reps 6-7 and reps 14-15.

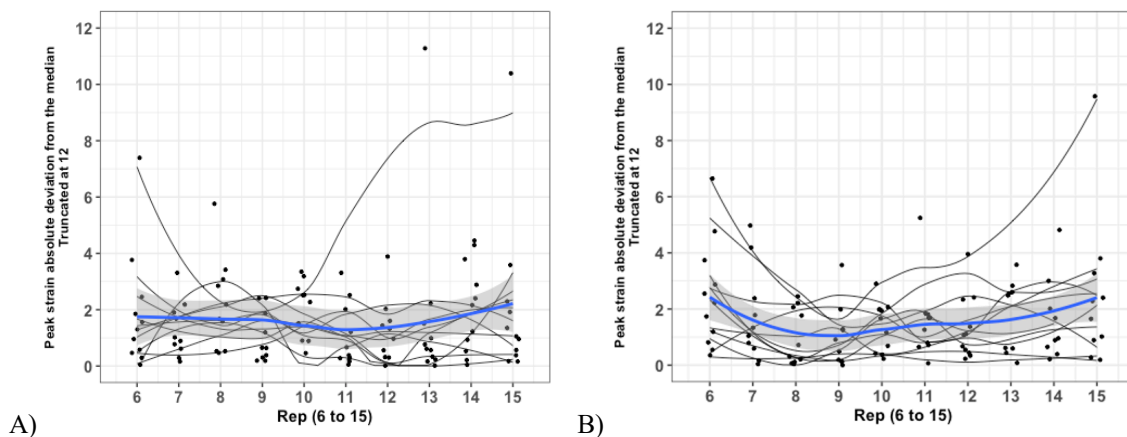


Figure 12. Trend in the absolute deviation around the median for **peak strain** over reps 6 to 15 for the **collagenase condition** – truncated figure (A) and **saline condition** – truncated figure (B)

Figure 12 shows trends in the absolute deviation around the median for peak strain in the collagenase and saline conditions. Based on maximum peak strain collagenase truncated data (N = 105 observations), there was not a significant quadratic trend over reps 6 to 15 (p-value = 0.26; R-squared = 1.5%) nor a significant linear trend over reps (p-value = 0.61; R-squared = 0.2%). Therefore, there is no evidence of a change in the repeatability over reps. Based on maximum peak strain saline truncated data from Examiner 2 (N = 103 observations), there was a significant quadratic effect over reps 6 to 15 (p-value = 0.006; R-squared = 7.7%). There is some evidence of change in the repeatability over reps with the repeatability being worst at reps 6-7, better around reps 8 and 9, and worsening from rep 10 to 15.

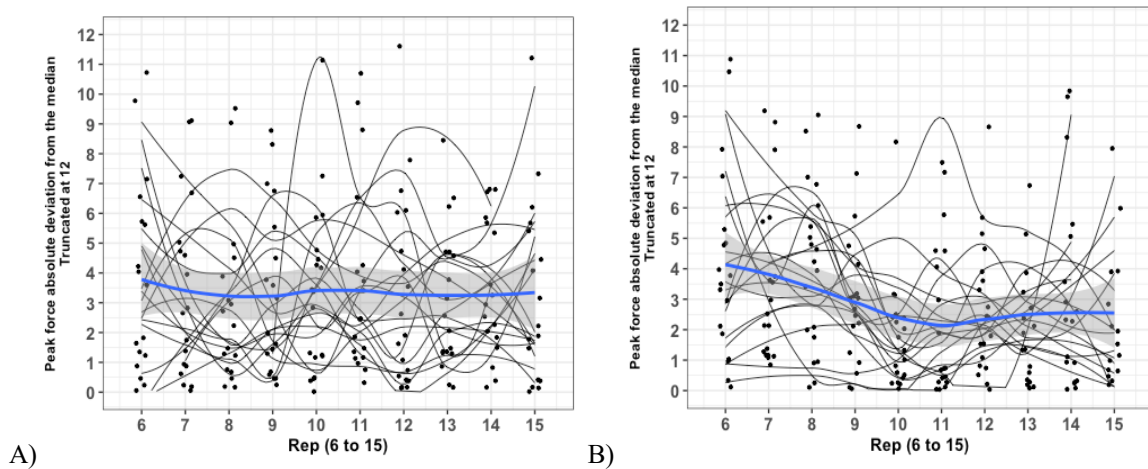


Figure 13. Trend in the absolute deviation around the median for **peak force** over reps 6 to 15 for the **dry condition** – truncated figure (A) and **saline condition** – truncated figure (B)

Figure 13 shows trends in the absolute deviation around the median for peak force in the dry and saline conditions. Based on maximum peak force dry test truncated data (N = 178 observations due to two outliers), there was not a significant quadratic trend over reps 6 to 15 (p-value = 0.70; R-squared = 0.1%). Also, there was not a significant linear trend over reps (p-value = 0.69; R-squared = 0%), indicating there is no evidence of a

change in the repeatability of force over reps. Based on all maximum peak force saline test data from Examiner 1 (N = 190 observations), there was a significant quadratic trend over reps 6 to 15 (p-value = 0.016; R-squared = 4.5%). Based on truncated data (N = 178 observations), there was a significant quadratic trend over reps 6 to 15 (p-value = 0.047; R-squared = 5.8%). There is some evidence of change in the repeatability of force over reps with the repeatability being better around rep 11 and worst at reps 6-8.

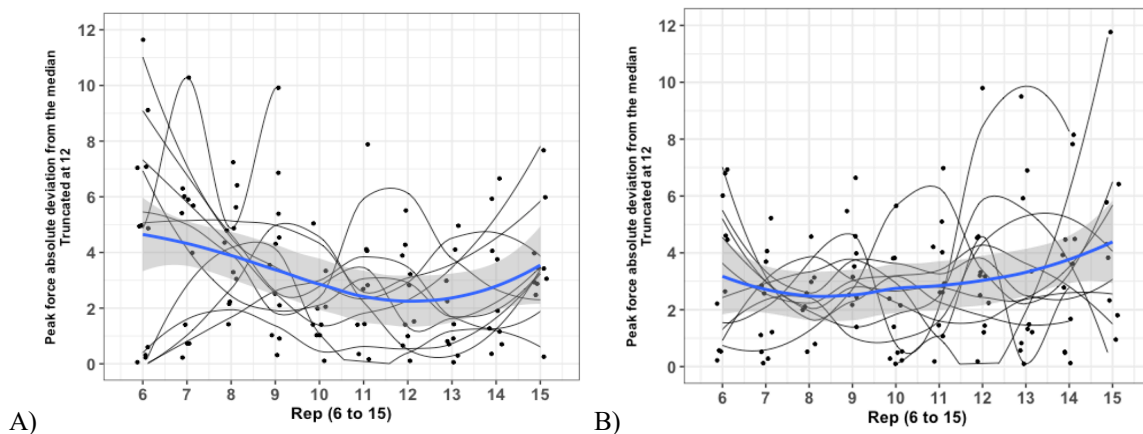


Figure 14. Trend in the absolute deviation around the median for peak force over reps 6 to 15 for the collagenase condition – truncated figure and saline condition – truncated figure (B)

Figure 14 shows trends in the absolute deviation around the median for peak force in the collagenase and saline conditions. Based on maximum peak force collagenase truncated data (N = 102 observations), there was not a significant quadratic trend over reps 6 to 15 (p-value = 0.076; R-squared = 9.8%), but there was a significant linear trend over reps (p-value = 0.010; R-squared = 5.6%). There is some evidence of change in the repeatability over reps with the repeatability being better around reps 12 and 13 and worst at reps 6-7. Based on maximum peak force saline truncated data from Examiner 2 (N = 101 observations), there was not a significant quadratic trend over reps 6 to 15 (p-value = 0.14; R-squared = 5.1%) nor a significant linear trend over reps (p-value = 0.15; R-

squared = 2.6%). The evidence of a change in the repeatability over reps was not statistically significant.

Trends over reps 6-15 in peak strain and peak force

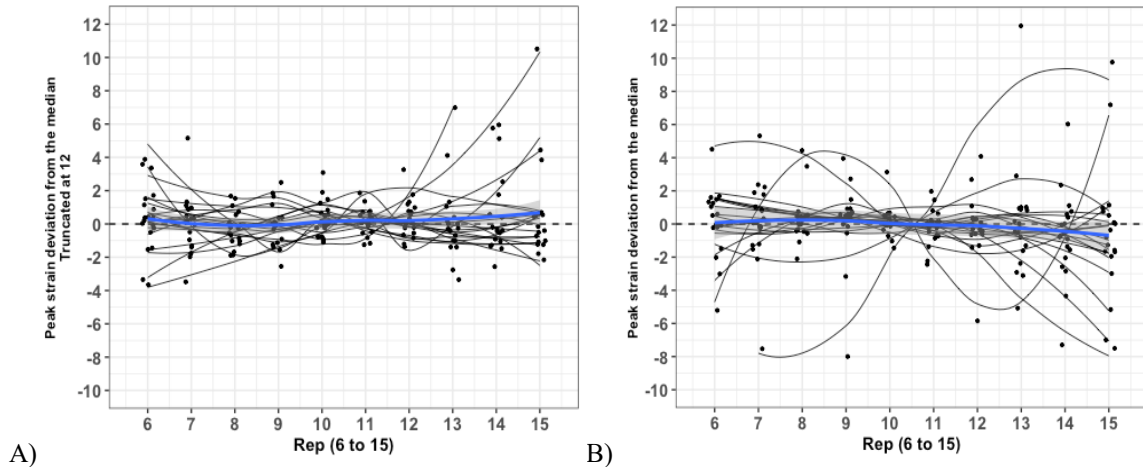


Figure 15. Trend in the deviation around the median for **peak strain** over reps 6 to 15 for the **dry condition** – truncated figure (A) and for the **saline condition** (B)

To evaluate if the repeatability of the peak strain and peak force measurements varied over reps 6 to 15, the deviation from the median within a trial was computed for each observation and plotted against the rep number. Figure 15 shows the trend in the deviation around the median for peak strain in the dry and saline conditions. Based on maximum peak strain dry test truncated data (N = 188 observations), there was not a significant quadratic trend over reps 6 to 15 (p-value = 0.34; R-squared = 1.4%) nor a significant linear trend over reps (p-value = 0.56; R-squared = 0.8%). Therefore, there is no evidence of a change in the peak strain over reps. Based on all maximum peak strain saline test data from Examiner 1 (N = 190 observations), there was not a significant quadratic trend over reps 6 to 15 (p-value = 0.69; R-squared = 0.8%), nor a significant linear trend over reps (p-value = 0.63; R-squared = 0.8%). There were no extreme

outliers and there is no evidence of a change in the peak strain over reps in the saline condition.

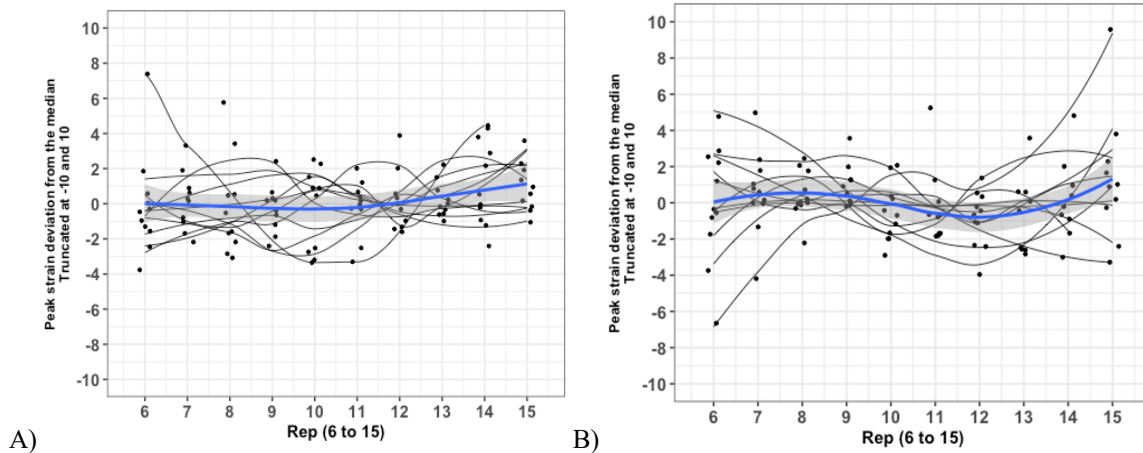
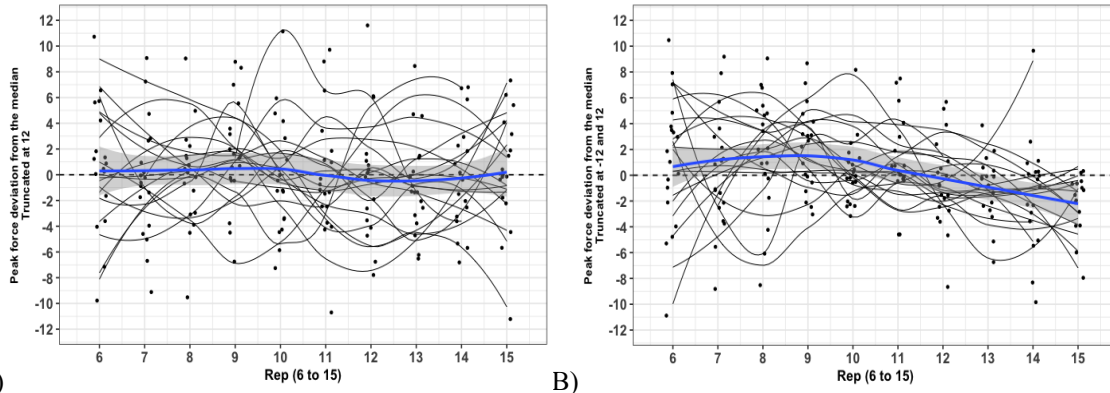


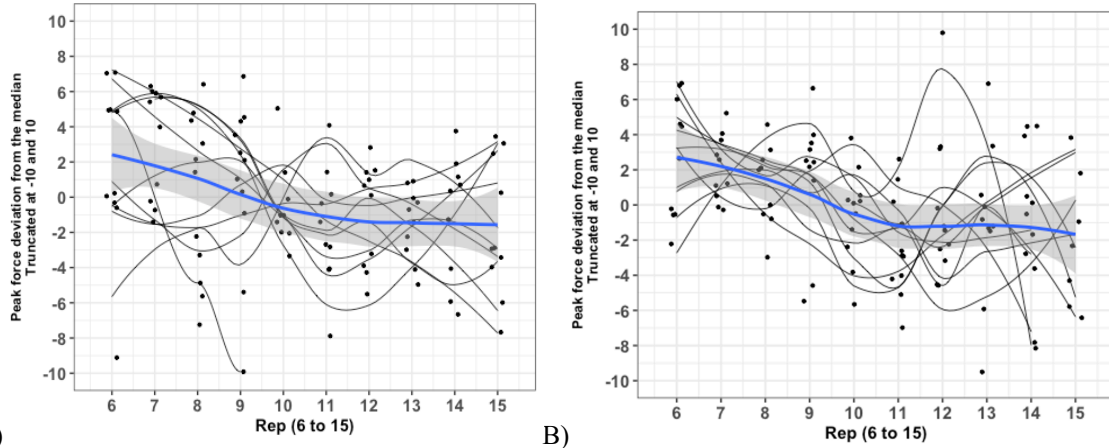
Figure 16. Trend in the deviation around the median for peak strain over reps 6 to 15 for the collagenase condition – truncated figure (A) and saline condition- truncated figure (B)

Figure 16 shows the trend in deviation around the median for peak strain for the collagenase and saline conditions. Based on maximum peak strain collagenase truncated data (N = 103 observations), there was not a significant quadratic trend over reps 6 to 15 (p-value = 0.33; R-squared = 5.1%) nor a significant linear trend over reps (p-value = 0.21; R-squared = 3.0%). From the truncated data there is no evidence of a change in the peak strain over reps. Based on maximum peak strain saline truncated data from Examiner 2 (N = 103 observations), there was not a significant quadratic trend over reps 6 to 15 (p-value = 0.17; R-squared = 2.5%). Also, there was not a significant linear trend over reps (p-value = 0.96; R-squared = 0.0%) indicating there is no evidence of a change in the peak strain over reps.



A) Figure 17. Trend in the deviation around the median for peak force over reps 6 to 15 for the dry condition – truncated figure (A) and for the saline condition – truncated figure (B)

Figure 17 shows the trend in the deviation around the median for peak force in the dry and saline conditions. Based on maximum peak force dry test truncated data (truncated at 12; N = 178 observations), there was not a significant quadratic trend over reps 6 to 15 (p-value = 0.87; R-squared = 0.2%), nor a significant linear trend over reps (p-value = 0.70; R-squared = 0.2%). Therefore, there is no evidence of a change in the peak force over reps in the dry condition. Based on maximum peak force saline test truncated data from Examiner 1 (truncated at -12 and 12; N = 180 observations), there was not a significant quadratic trend over reps 6 to 15 (p-value = 0.095; R-squared = 9.4%). However, there was a significant linear trend over reps (p-value = 0.0032; R-squared = 7.4%). Based on the truncated data there is some evidence that peak force was decreasing over the reps.



A) Figure 18. Trend in the deviation around the median for peak force over reps 6 to 15 for the collagenase condition – truncated figure (A) and for the saline condition – truncated figure (B)

Figure 18 shows the trend in the deviation around the median for peak force in the collagenase and saline conditions. Based on maximum peak force collagenase truncated data (N = 100 observations), there was not a significant quadratic trend over reps 6 to 15 (p-value = 0.29; R-squared = 12.9%), but there was a significant linear trend over reps (p-value = 0.0496; R-squared = 11.7%). There is some evidence that the peak force was decreasing over reps. Based on maximum peak force saline truncated data from Examiner 2 (N = 100 observations), there was not a significant quadratic trend over reps 6 to 15 (p-value = 0.36; R-squared = 15.5%), but there was a significant linear trend over reps (p-value < .001; R-squared = 14.1%), showing on the truncated data there is some evidence that peak force was decreasing over the reps.

DISCUSSION

FBG strain measurements detected changes in fiber conditions within the PDL space but differences due to fluid content were more difficult to distinguish. As can be seen in Table 4, the median peak strain and force difference between the dry and saline conditions did not reach statistical significance. However, the upper bound of 95% CI

was 0.11 for the peak strain, close to zero, which suggests strain may be somewhat lower for the dry condition as could be explained due to the absence of liquid movement within the PDL upon displacement at similar peak forces. Comparing the saline and collagenase samples, as seen in Table 5, the saline samples had greater maximum peak strain values than saline w/ collagenase but no difference in the force values. These greater strain values in specimens with intact PDL fibers are evidence that the FBG sensor can be used to detect the capacity of the ligament to deform when loaded. The greater saline strain values may be explained as the PDL fibers are present and transmit the force applied to the tooth into strain within the fibers. The PDL fibers also create more interference with liquid flow and may deter the replenishment of fluids in the tissue after each test. In contrast, when the PDL fibers have been depleted following the fiberotomy and collagenase incubation, no load transmission can occur, and only fluid movement may contribute to FBG deformation. This is consistent with an in-vitro rat model that also compared periodontal biomechanics in intact vs. collagenase depleted ligaments (Komatsu, 2007a). Also seen in a previous rat study using subcutaneous human relaxin administration, it was found that while relaxin does not accelerate orthodontic tooth movement, it can reduce the level of PDL organization, reduce PDL mechanical strength, and increase initial tooth mobility (Madan et al., 2007), thus suggesting that the viscoelastic properties of collagen fibers within the PDL may play an important role in the stress-relaxation process.

The time-dependent viscoelastic response of the PDL was detected using FBG strain measurements. The order of which dry or saline testing condition was performed first did not affect the maximum peak strain or force values as seen in Table 6. However,

there is some evidence that the repeatability of both peak force and peak strain was better for the 1st set of reps regardless of condition as the 95% CI is close to zero. With repeated loading, some consequences can be breakage of the tooth or FBG sensor, breakdown of the collagen fibers within the PDL space or slight movement of the specimen that could affect measured readings over time.

The repeatability of tests was lower in specimens with intact PDL fibers in saline conditions. The absence of fluid, i.e. dry condition or fibers i.e. collagenase/fiberotomy condition resulted in a trend toward an increase in strain repeatability. Comparing the maximum peak strain and force median absolute deviation (MAD) values for repeatability in the dry vs. saline conditions and saline vs. collagenase conditions showed no statistical difference (Table 7 & 8). However, as the 95% CI was close to zero for strain, there is some evidence that the dry and collagenase samples had greater repeatability than saline. This can be explained by fluid movement and alteration in the PDL fibers with repeated load over time. As a result, in living tissue, the cells within the PDL space experience greater variability in strain levels and may undergo functional changes. Studies on in-vitro fibroblasts have shown the cells to be strain sensitive and to respond with altered expression of growth factors dependent on the magnitude of mechanical strain induced (Jacobs, 2013 and Jin et al., 2020). This adaptability of cellular and fiber responses may explain how strain variation may occur over time during the intermittent repeated loads of mastication or the use of elastics with repeated load on teeth to aid in orthodontic tooth movement. Every individual is unique with varying fluid, fiber and cellular content within the PDL and the stress relaxation of fibers and

cellular changes may be responsible for differing responses to orthodontic loads such as the amount of time needed for space closure or ability to de-rotate teeth.

Age differences in FBG strain measurements were not detected. The absence of differing peak force and strain measurements between the younger and older pig samples could reflect the PDL's capacity to adapt to increases in load associated with growth, such as increased masticatory forces. As two age group specimens were tested, Table 2 shows no difference in repeatability in the peak force and strain for the saline condition so both age groups were pooled for data analysis. No significant differences were noted in the values for the young pig saline condition between Examiner 1 and 2, validating data from both examiners through consistency in methodology (Table 3).

A quadratic trend over reps 6-15 was seen for peak strain MAD for both dry and saline conditions (Figures 11A & B) and highlight the potential for changes in PDL fibers to occur during repeated loading. In dry and saline conditions, similar changes in repeatability occurred with the least deviation from the median around reps 10-11, i.e. in the middle of the sequence. Thus, varying strain readings may be explained with early variation resulting from continued preconditioning of the specimen and later variation to be fatigue in the tissues as the tooth may be able to withstand only so much force before the fibers become weakened or altered. These changes in PDL strain are relevant to orthodontic movement in that being able to know how often and the amount of force applied that is necessary to generate a specific PDL strain will give more control and precision in movement. The collagenase samples did not exhibit a quadratic or linear trend indicating no evidence of change in the repeatability over reps (Figure 12). Due to the reduction of PDL fibers, the collagenase strain values remained more consistent as

there is no cushioning effect on the transmission of force as seen with the fibers present, therefore no longer having viscoelastic properties.

A significant force trend was noted between conditions. While the peak force for the dry condition exhibited no statistical difference over the reps, both the saline and collagenase had a significant linear downward trend showing evidence of decreasing peak force over time (Figures 17 and 18). This finding is consistent with the time-dependent behavior of the PDL as seen in previous studies on in-vitro swine model showing increase in loading time forces fluid to flow into surrounding periodontal tissues resulting in a decrease in measured forces (Knaup et al., 2018 and Papadopoulou et al., 2014). For both the saline and collagenase-treated specimens, saline was able to flow freely within the PDL space and allowed a 5-minute rest between reps to allow fluid to return. This decrease in force may be explained by fatigue within the PDL as an intermittent force is applied, not allowing the fibers to recoil and relax back to its original position, therefore requiring less force to induce an intrusive 0.5mm change. This can be applicable to orthodontic tooth movement in that less force is needed to induce a change in tooth position with repeated application over time, therefore not over-stressing the biological components that could lead to adverse unwanted effects.

One of the limitations with this study is using an ex-vivo sample of pig teeth, as FBG measurements of periodontal strain need to be better understood before in-vivo experiments on pig or human teeth can be performed. While pigs are a good animal model, pig teeth are biologically more robust than human due to differences in periodontal structure with greater root length, making the pig periodontal tissues very resistant to load. The FBG sensor was placed to a premeasured 10mm depth for all

incisors of both age groups, however without a 3-D radiograph, the exact position of the sensor along the root cannot be determined and varying location along the root may affect FBG strain readings. With the two different age groups, there is expected to be variation in root length with the older group having longer roots, greater bone density and maturation of the PDL (Tonge and McCance, 1973), all which can potentially affect strain and force readings. The incisor roots also have a slight lingual curve in the alveolar housing, so the long-axis of the tooth is difficult to accurately determine, and each tooth is individual with distinct anatomy. The positioning of the teeth relative to the loading platen resulted in varying magnitude measurement readouts of strain from the SmartScan, outputting positive compression values and negative tension values. There were therefore no consistent values that could be compared between specimens, so each incisor was analyzed individually and independently for the peak strain and force.

All younger pigs were obtained from the UW paramedical training facility and older pigs from one local butcher therefore from two different sources and the exact age of the animals cannot be determined. Due to selective animal sources and the inability to collect specimens for several months due to Covid-19, there was a limit to the number of incisors to be tested. The fibrotomy with collagenase tests were originally performed on the young pigs, however, due to their small size, following incubation with collagenase, some of the incisors were very loose and a repeatable reading could not always be acquired from the fiberoptic sensor due to the unstable teeth. Therefore, the older pigs of larger size were obtained all from the same butcher and proved to be more robust with greater alveolar support to withstand the collagenase and incubation period, allowing for proper FBG placement and testing. Due to the time needed for each saline vs.

collagenase experiment, following the saline reps and collagenase incubation, the specimen was stored submerged in saline overnight in the refrigerator. The FBG was removed from the PDL for fibrotomy and collagenase incubation, therefore exact positioning of the sensor in the same incisor could not be replicated between the saline and collagenase trials which may have affected strain readings. The saline vs. collagenase tests had a limited sample due to procurement issues so it is under powered. Due to the size and composition of the FBG sensors, they are fragile and are technique sensitive to become proficient in adequate placement within the PDL, however both examiners did have reliable strain readings.

This research study focused primarily on incisor teeth, as a future goal is to implement this technique in living pigs and subsequently human teeth. While the better model would be to test premolar and molar teeth to compare with human teeth, accessibility of incisors in the pig is a major factor for choosing to focus on the anterior region of the mandible.

Testing samples on ex-vivo specimens is necessarily different than in the in-vivo environment. For example, changes in proteoglycan content and molecular weight that occur during normal inflammatory and periodontal healing processes cannot be accounted for. Also, only an apical, intrusive load was applied to these teeth; thus, these studies will not model what occurs orthodontically with extrusive, lateral, and rotational forces.

CONCLUSION

FBG sensors were effective in producing strain readings in swine incisor teeth when an intrusive load was applied at the incisal edge. Findings that were statistically significant include greater peak strain value readings from the saline group relative to the collagenase group. More consistency was noted in FBG strain readings in dry and collagenase specimens compared to saline and in the first set of reps for each test regardless of condition. There was also a noted downward force trend for both the saline and collagenase-treated specimens. In conclusion, allowing fluid flow within the PDL space produced greater strain than when dry and even more so with the absence of collagen fibers. The force needed over time to intrude the incisor 0.5mm decreased with additional repetitions which may provide insight in the amount of load required to orthodontically move a tooth effectively and reducing negative side effects.

ACKNOWLEDGEMENTS

I would like to thank Isabelle Hwang for her contribution to this project by collecting data for the saline vs. collagenase trials. In addition, I would like to thank our collaborators, Kathryn Houg and Dr. Dan Romanyk from the University of Alberta for their assistance in methodology and knowledgeable input in FBG sensor use. This project would not have been possible without the continual guidance of Dr. Tracy Popowics throughout this process and Dr. Sue Herring for the use of equipment, lab space, and her expertise. I would also like to thank Dr. Anne-Marie Bollen and Dr. Katherine Rafferty's supportive input as part of my thesis committee, and Dr. Lloyd Mancl for his comprehensive statistical analysis. This project was supported by the

University of Washington Orthodontic Alumni Association and the American Association of Orthodontists Foundation.

LITERATURE CITED

- Al-Fakih, E., Osman, N. A. A. and Adikan, F. R. M (2012). 'The use of fiber bragg grating sensors in biomechanics and rehabilitation applications: The state-of-the-art and ongoing research topics.' *Sensors*, 12, pp. 12890-12926.
- Al-Rekabi, Z., Fura, A., Juhlin, I., Yassin, A., Popowics, T., & Sniadecki, N. (2019). 'Hyaluronan-CD44 interactions mediate contractility and migration in periodontal ligament cells.' *Cell Adhesion & Migration*, 1-13.
- Beertsen, W., McCulloch, C., & Sodek, J. (1997). 'The periodontal ligament: A unique, multifunctional connective tissue.' *Periodontology*, 2000, 13(1), 20-40.
- Bergomi, M., Wiskott, H., Botsis, J., Mellal, A., Belser, U. (2010). 'Load response of periodontal ligament: assessment of fluid flow, compressibility, and effect of pore pressure.' *Journal of Biomechanical Engineering-Transactions of the Asme*, 132(1), 1-5.
- Bergomi, M., Cugnoni, J., Botsis, J., Belser, U., Wiskott, H. (2010B). 'The role of the fluid phase in the viscous response of bovine periodontal ligament.' *Journal of Biomechanics*, 43(6), 1146-1152.
- Berkovitz, B. (1990). 'The structure of the periodontal ligament: An update.' *European Journal of Orthodontics*, 12(1), 51-76.
- Brezniak, N. & Wasserstein, A. (1993). 'Root resorption after orthodontic treatment: Part 1. Literature review.' *American Journal of Orthodontics & Dentofacial Orthopedics*, 103(1), 62-66.
- Canty, A. and Ripley, B. (2019). *boot: Bootstrap R (S-Plus) Functions*. R package version 1.3-24.
- Cheng, Türk, Elekdağ-Türk, Jones, Yu, & Darendeliler. (2010). 'Repair of root resorption 4 and 8 weeks after application of continuous light and heavy forces on premolars for 4 weeks: A histology study.' *American Journal of Orthodontics & Dentofacial Orthopedics*, 138(6), 727-734.
- Cleveland, W. S. (1979). 'Robust locally weighted regression and smoothing scatterplots.' *Journal of the American Statistical Association*, 74, 829-836.

- Cusano, A., Cutolo, A., & Albert, J. (2011). Fiber Bragg grating sensors recent advancements, industrial applications and market exploitation. Saif Zone, Sharjah, United Arab Emirates]: Bentham Science.
- Davison, A. C. & Hinkley, D. V. (1997). *Bootstrap Methods and Their Applications*. Cambridge University Press, Cambridge. ISBN 0-521-57391-2.
- Faul, F et al. (2007). 'Experimentally determined mechanical properties of, and models for, the periodontal ligament: critical review of current literature.' *Journal of Dental Biomechanics*, 2011, p. 10 Pages.
- Hardin, J. & Hilbe, J. (2003). *Generalized Estimating Equations*. London: Chapman and Hall/CRC. ISBN 978-1-58488-307-4.
- Henneman, S., Von den Hoff, J., & Maltha, J. (2008). 'Mechanobiology of tooth Movement.' *The European Journal of Orthodontics*, 30(3), 299-306.
- Højsgaard, S., Halekoh, U. & Yan J. (2006) The R Package geepack for Generalized Estimating Equations *Journal of Statistical Software*, 15, 2, pp1—11.
- Jacobs, C., Grimm, S., Ziebart, T., Walter, C., & Wehrbein, H. (2013). 'Osteogenic differentiation of periodontal fibroblasts is dependent on the strength of mechanical strain.' *Archives of Oral Biology*, 58(7), 896-904.
- Jin, Y., Ding, L., Ding, Z., Fu, Y., Song, Y., Jing, Y., Li, Q., Zhang, J., Ni, Y., Hu, Q. (2020). 'Tensile force-induced PDGF-BB/PDGFR β signals in periodontal ligament fibroblasts activate JAK2/STAT3 for orthodontic tooth movement.' *Scientific Reports*. 10(1):11269.
- Kitaura, H., Kimura, K., Ishida, M., Sugisawa, H., Kohara, H., Yoshimatsu, M., & Takano-Yamamoto, T. (2014). 'Effect of cytokines on osteoclast formation and bone resorption during mechanical force loading of the periodontal membrane.' *The Scientific World Journal*, 2014, 7.
- Knaup, T.J., et al (2018). 'Time-dependent behavior of porcine periodontal ligament: A combined experimental, numeric in-vitro study.' *American Journal of Orthodontics and Dentofacial Orthopedics*, 153: 97-107).
- Kohara, H., Kitaura, H., Yoshimatsu, M., Fujimura, Y., Morita, Y., Eguchi, T., & Yoshida, N. (2012). 'Inhibitory effect of interferon-[gamma] on experimental tooth movement in mice.' *Journal of Interferon & Cytokine Research*, 32(9), 426-31.
- Komatsu, K., Shibata, T., & Shimada, A. (2007a). 'Analysis of contribution of collagen fibre component in viscoelastic behavior of periodontal ligament using enzyme probe.' *Journal of Biomechanics*, 40(12), 2700-6.

- Komatsu, K. et al (2007b). 'Stress-relaxation and microscopic dynamics of rabbit periodontal ligament.' *Journal of Biomechanics*, 40(3), 634-644.
- Komatsu, K. (2010). 'Mechanical strength and viscoelastic response of the periodontal ligament in relation to structure.' *Journal of Dental Biomechanics*, 502138. Doi: <https://doi.org/10.4061/2010/502318>.
- Levander, E. & Malmgren, O. (2000). Long-term follow-up of maxillary incisors with severe apical root resorption. *European Journal of Orthodontics*, 22(1), 85-92.
- Maeda, Y., Kuroda, S., Ganzorig, K., Wazen, R., Nanci, A., & Tanaka, E. (2015). 'Histomorphometric analysis of overloading on palatal tooth movement into the maxillary sinus.' *American Journal of Orthodontics & Dentofacial Orthopedics*, 148(3), 423-430.
- Measures, R. (2001). *Structural Monitoring with Fiber Optic Technology*. 1st Edition. Academic Press.
- Natali, A. N. et al. (2004). 'Viscoelastic response of the periodontal ligament: An experimental-numerical analysis.' *Connective Tissue Research*, 45(4), 222-230.
- Oltramari, P., Navarro, R., Henriques, J., Capelozza, A., & Granjeiro, J. (2007). 'Dental and skeletal characterization of the BR-1 minipig.' *The Veterinary Journal*, 173(2), 399-407.
- Quinn, R. & Yoshikawa, D. (1985). 'A reassessment of force magnitude in Orthodontics.' *American Journal of Orthodontics*, 88(3), 252-260.
- Papadopoulou, K., Hasan, I., Keilig, L., Reimann, S., Eliades, T., Jäger, A., Bourauel, C. (2013). 'Biomechanical time dependency of the periodontal ligament: A combined experimental and numerical approach.' *European Journal of Orthodontics*, 35(6), 811-818.
- Papadopoulou, K., Keilig, L., Eliades, T., Krause, R., Jager, A., Bourauel, C. (2014). 'The time-dependent biomechanical behavior of the periodontal ligament – an in vitro experimental study in minipig mandibular two-rooted premolars.' *European Journal of Orthodontics*, 36, 9-15.
- Patterson, A., & Popowics, T. (2014). 'Experimental ex vivo traumatic intrusion in the mandibular incisors of the farm pig, *Sus scrofa*.' *Dental Traumatology*, 30(6), 423-428.
- Popowics, T., Rensberger, J., & Herring, S. (2004). 'Enamel microstructure and microstrain in the fracture of human and pig molar cusps.' *Archives of Oral Biology*, 49(8), 595-605.

- R Core Team (2020). R: A language and environment for statistical computing. R Foundation for Statistical Computing, Vienna, Austria. URL <https://www.R-project.org/>.
- Romanyk, D., Guan, R., Major, P., & Dennison, C. (2017). 'Repeatability of strain magnitude and strain rate measurements in the periodontal ligament using fibre Bragg gratings: An ex vivo study in a swine model.' *Journal of Biomechanics*, 54, 117-122.
- Takahashi, I., Nishimura, M., Onodera, K., Bae, J., Mitani, H., Okazaki, M., & Sasano, Y. (2003). 'Expression of MMP-8 and MMP-13 genes in the periodontal ligament during tooth movement in rats.' *Journal of Dental Research*, 82(8), 646-651.
- Takahashi, I., Onodera, K., Nishimura, M., Mitani, H., Sasano, Y., & Mitani, H. (2006). 'Expression of genes for gelatinases and tissue inhibitors of metalloproteinases in periodontal tissues during orthodontic tooth movement.' *Journal of Molecular Histology*, 37(8), 333-342.
- Toms, S., Dakin, G., Lemons, J., & Eberhardt, A. (2002). 'Quasi-linear viscoelastic behavior of the human periodontal ligament.' *Journal of Biomechanics*, 35(10), 1411-1415.
- Tonge, C. H., & McCance, R. A. (1973). 'Normal development of the jaws and teeth in pigs, and the delay and malocclusion produced by calorie deficiencies.' *Journal of anatomy*, 115(Pt 1), 1-22.
- Viecilli, R., Katona, T., Chen, J., Hartsfield, J., & Roberts, W. (2009). 'Orthodontic mechano-transduction and the role of the P2X7 receptor.' *American Journal of Orthodontics and Dentofacial Orthopedics*, 135(6), 694-695.
- Viecilli, R., Kar-Kuri, M., Varriale, J., Budiman, A., & Janal, M. (2013). 'Effects of initial stresses and time on orthodontic external root resorption.' *Journal of Dental Research*, 92(4), 346-351.
- Wei, Z et al. (2014). 'Experiment and hydro-mechanical coupling simulation study on the human periodontal ligament.' *Computer Methods and Programs in Biomedicine*, 113(3). 749-756.
- Zhang, L., Liu, W., Zhao, J., Ma, X, Shen, L., Zhang, Y., Jin, F., Jin, Y. (2016). 'Mechanical stress regulates osteogenic differentiation and RANKL/OPG ratio in periodontal ligament stem cells by the Wnt/ β -catenin pathway.' *Biochimica et Biophysica Acta*, 1860(10), 2211-2219.